SÍSMICA 2024 13º Congresso Nacional de Sismologia e Engenharia Sísmica

COMPREHENSIVE MULTI-RISK ASSESSMENT FOR THE LISBON METROPOLITAN AREA

GLENDA MASCHERI
PhD Student
Universidade do Minho

NICOLA CHIEFFO
Post-Doctoral Researcher
Universidade do Minho

XAVIER ROMÃO
Assistant Professor
FEUP

PAULO B. LOURENÇO
Full Professor
Universidade do Minho

ABSTRACT

The significance of dealing with multiple risks has become increasingly clear given the rising frequency of disasters caused by natural and man-made hazards impacting metropolitan areas. The current study focuses on an urban structural compound within the Lisbon Metropolitan Area (LMA) and the primary goal is to evaluate the vulnerability and risk associated with both earthquakes and flooding, respectively. It includes multi-vulnerability models that are adapted to specific threats, taking into consideration elements like water depth and earthquake damage. Subsequently, the study involves the development of typological fragility curves and explores the correlation between seismic and rainfall-induced damages. The main outcomes of this research provide an opportunity to enhance emergency preparedness by fostering increased collaboration among rescue organizations and government agencies involved in disaster management. Furthermore, the research highlights the limitations of the proposed approach and provides important insights for future developments regarding the interdependence of the considered hazards.

KEY-WORDS: Multi-risk assessment, Earthquake vulnerability, Flood vulnerability, Fragility curves, Loss estimation.

1. INTRODUCTION

Disasters have risen in importance in recent decades since they represent severe concerns all over the world, leading to an increase not just in monetary losses, but also in service interruption and mortality. These disasters are expected to become more frequent and severe in the next decades, due to factors such as climate change, growth in population, uncontrolled urbanisation, and inadequate governance at all levels [1], [2].To provide some context, [3] reported that, between 1985 and 2014, disasters increased yearly economic losses from $14 billion to more than $140 billion. The same document reported that throughout the decade 2005-2015, weather-related events caused the highest economic loss, with floods accounting for 30.5% of total losses, followed by multi-hazard catastrophes (14.4%) and earthquakes (12.5%), indicating that earthquakes and floods are two hazards that must be addressed. The term risk can be defined as "*the combination of the probability of an event and its negative consequences*" [4] and it can normally be evaluated as a convolution of hazard (H), vulnerability (V) and exposure (E) [5]. However, it has been recognised by several authors [1], [6]–[9] that, when a site is frequently struck by multiple hazards, an effective disaster risk reduction may be achieved if all threats are evaluated jointly, giving rise to a multi-hazard perspective. The interest in multi-hazard began with the Agenda 21 Conference in Rio de Janeiro [10] and the Johannesburg Declaration of Sustainable Development [11], which started to highlight the importance of a comprehensive multi-hazard approach aimed at risk reduction that includes vulnerability and risk assessment, as well as all phases of disaster management, including prevention, mitigation, preparedness, response, and recovery, as depicted in [7]. Later on, these concepts were reaffirmed in the Hyogo Framework for Action, HFA [12], and in the UN Sendai Framework for Disaster Risk Reduction 2015-2030 [13]. However, risk awareness and risk assessment are critical not only for preventing losses and protecting ecosystems and human lives but also for preserving historical city centres. Indeed, city centres must be protected given their blend of tangible and intangible values: their economic worth, but also for the historical importance, social identity, and immaterial significance to communities [2], [14]. While there are multiple methods for measuring vulnerability and risk due to the importance of risk mitigation, only a few examine multiple hazards at the same time, and even less address the specifi issues of historical centres [2], [6], [15]. Addressing this multi-hazard problem and developing the necessary metrics to estimate vulnerability and losses involves several technical and financial challenges. Furthermore, there are additional issues related to the interrelationships generated by the spatial and temporal overlap of distinct hazards that will alter the global level of risk. Hence, the multi-hazard effects are likely to differ from the sum of the single-hazard impacts. All of these issues are amplified in old city centres, where the complexity of the physical environment accentuates the challenges to achieve their preservation [1], [2], [6], [16]. Given the difficulty of the topic, several literature studies on multi-hazard approaches have attempted to clarify the general framework of the multi-hazard context [1], [6], [8], [15], [16]. Following the subdivision made by [6], existing methods can be grouped into multi-hazard analysis, vulnerability to multiple hazards analysis, and multi-hazard risk analyses. In multi-hazard analysis, the likelihood of several hazards occurring is estimated [17], [18]. As seen in [19], and [20], the vulnerability to multiple hazards is calculated taking into account that one hazard can change the vulnerability for the subsequent one or that the same vulnerability characteristics can contribute differently to different hazards. The multi-hazard risk analysis is a combination of the two preceding processes [5], [21].

In light of these considerations, the goal of the current study is to develop a comprehensive multi-risk assessment method that is particularly designed for historical centres. Specifically, the case study will assess the vulnerability and risk of typical unreinforced masonry structures (URM) to floods and earthquakes in a neighbourhood of Lisbon that has already experienced these types of events [22], [23]. The exposure model was developed using remote sensing methods and then integrated into the GIS

environment. Seismic and flood vulnerability were evaluated using the Risk-UE approach and existing flood state-damage curves, respectively.

Next, damage scenarios for different return periods were simulated to provide a global overview of the assets exposed to risk. Finally, a comprehensive multi-risk assessment was carried out, which included an evaluation of the building's economic losses. This method provides a comprehensive view of evaluating the global economic impact induced by the above-introduced hazards on the case study building stock.

2. CASE STUDY AREA

As previously mentioned the case study focused on a specific neighbourhood of Lisbon, notably the downtown area. Lisbon, the capital of Portugal, is situated in the country's southernmost region along the north bank of the Tagus River estuary. The Lisbon downtown, namely Baixa Pombalina, is a riverfront neighbourhood that has historical relevance in the city's disaster history. To this day, it is a tourist attraction where tourists can learn about the cultural identity and history of the city [24], and it has been subjected to a historical preservation plan known as Plano de Pormenor de Salvaguarda da Baixa Pombalina (PPSBP) since 2011, as depicted in [25]. The focus of the case study (Fig. 1), is an area enclosed by the Rua Nova do Almada (West), Praça Dom Pedro IV and Praça da Figueira (North), Rua da Madalena (East) and Praça do Comércio (South).

Fig. 1 – Case study area. Adapted from [26].

This area holds particular historic significance due to its association with the "Great Lisbon earthquake" that occurred on November 1st, 1755. This devastating earthquake led to the area's destruction, which was further exacerbated by the subsequent tsunami and urban fires. In the aftermath of this tragedy, the Marquis of Pombal took charge of the area's reconstruction. Notably, this reconstruction introduced the distinctive "Pombalino" architectural style, characterized by its emphasis on sturdiness, uniformity, and regularity, all designed to enhance seismic resilience [23], [25]. The structural configuration of buildings in the Pombalino style included the so-called "Gaiola Pombalina", which can be described as a structure made up of a series of internal walls called "frontal" walls that have a three-dimensional timber structure forming a triangular geometry filled with poor quality masonry and are connected to the orthogonal walls by vertical studs in the corners. Typically, the façades and walls between two consecutive buildings are constructed using ordinary stone masonry. The structure, along with the timber flooring, ensures the bracing of the outside stone masonry walls and the resistance to forces in any direction [23], [25], [27]. The aforementioned area is made up of 393 ordinary buildings organized in aggregates. The analysed buildings sample in the area are unreinforced masonry structures (URM) erected in the "Pombalino" style (82%),

with several others (18%) in reinforced concrete (RC) as a consequence of interventions throughout the years. According to [25], the occupancy of these buildings is mostly mixed, with commercial activity on the ground floor and residential uses on the higher floors.

3. EXPOSURE MODEL

The exposure is defined as "*people, property, systems, or other elements present in hazard zones that are thereby subject to potential losses*" [4]. Exposure, together with the vulnerability, and capability of the exposed assets must be integrated to evaluate risks associated with a given hazard in the area of interest [28]. People, properties, economic activities, and private and public services are all examples of assets exposed to risk and they can all be affected directly or indirectly by a catastrophic occurrence in a particular location [29]. Building exposure is often characterized by its location and monetary value [2], and it is one of the most important spatial data layers to be employed for risk assessment [29]. When analysing risk, all assets that are potentially exposed to hazards must be identified, categorised, and organized in a georeferenced inventory that contains all their relevant attributes. In the current study, the exposure model was considered by gathering data about the investigated buildings that were subsequently used to develop a complete inventory in the QGIS environment [30]. The statistical distribution of the main building attributes, i.e. building typology, number of floors and physical condition, is reported in Fig. 2.

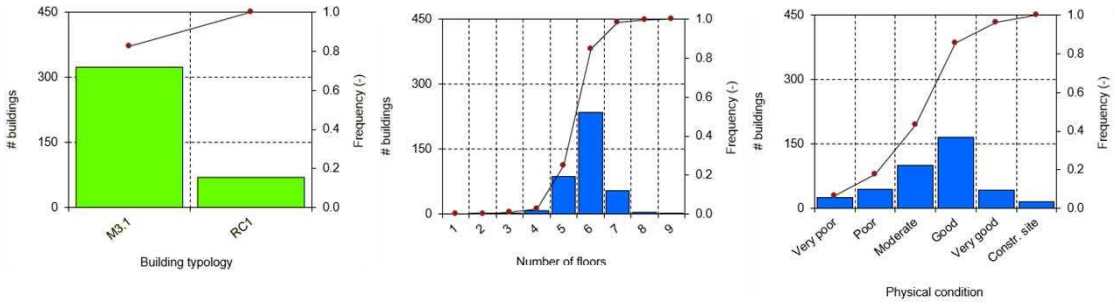

a) b) c)

Fig. 2 – Spatial distribution of main attributes for the study area: a) building typology; b) number of floors; c) physical condition.

Figure 2 illustrates that 82% of the building samples are URM, while 18% are made of RC. These buildings are from 2 to 9 floors in height, with a majority (96%, i.e. 376 buildings) having 5 to 7 floors. Concerning the physical condition, 53% of the sample is classified as good or very good, while a considerable percentage (42%) is in a moderate to very poor condition. In terms of aggregate location, which normally consists of an average of 8 buildings per aggregate, the intermediate category has the biggest proportion (58%), followed by the corner (37%), and a lower fraction of buildings categorised as head (5%). Regarding the monetary exposure of the buildings, it was calculated using the market values available at [31], which were 5200 €/m^2 for commercial areas and 3788 €/m^2 for residential areas. The following equation is then used to compute the monetary exposure of each building (E_i), where term A_j is the floor area, term $V_{m,j}$ is the market value, and term n_j is the number of floors:

$$E_i = \sum_{j=1}^{n} V_{m,j} \cdot A_j \cdot n_j \quad (1)$$

4. HAZARD MODEL

A hazard is "*a process, phenomenon or human activity that may cause loss of life, injury or other health impacts, property damage, social and economic disruption or environmental degradation*" [28]. Hazard models need to represent hazards using a measure of their intensity.

For earthquakes, seismic intensity can be described in various ways, with the most common metrics being macroseismic intensity or Peak Ground Acceleration (PGA) [32]. In the case of floods, the intensity measure is generally defined by adopting the water depth and the inundation extent that may be achieved during the flood event [2]. Therefore, in the current work, the seismic scenario was simulated using macroseismic intensity as the intensity measure. Concerning the flood scenario, it involved analysing the spatial extent of inundation and the corresponding water depths resulting from heavy rainfall-induced flood events.

4.1. Seismic hazard

Portugal has a moderate to high seismic hazard and has undergone high-intensity seismic activity throughout its history, resulting in the loss of many lives and buildings [23], [27]. Specifically, the city of Lisbon has experienced several devastating events due to its position on the border between the Eurasian and African plates, including the earthquake on 26th January 1531 (estimated magnitude $6.0<M_w<6.6$); the Benavente earthquake (1909), with an estimated magnitude M_w of 6.0; and the Algarve earthquake in 1969, an offshore earthquake with a magnitude M_w of 7.8 [23], [33], [34]. However, the most significant earthquake in Portugal was "The Great Lisbon Earthquake" in 1755 with an estimated magnitude of roughly 8.5 on the Richter scale, followed by the subsequent tsunami and fire events. In Lisbon, this event damaged around 85% of the structures, causing the loss of 30,000 to 40,000 lives [23]. The seismic hazard characterization of the city of Lisbon in the current study was based on the results of other seismic hazard studies. In particular, [35] defined a mean hazard map for Portugal with PGA in rock for a 10% exceedance probability in 50 years (i.e. return period of 475 years) ranging from 0.05g to 0.20g, with the highest PGA in the Lisbon and Algarve regions. Therefore a PGA of 0.20g for a return period of 475 years was chosen for Lisbon, and then all the associated PGA for other return periods (i.e. 5, 10, 20, 50, 100 years) were calculated through correlation equations reported in [36].

4.2. Flood hazard

In terms of flood hazard, the country has already seen some significant flood occurrences, such as those in November 1967, November 1983, and February 2008 [22], [37]–[39]. All of these events set a daily rainfall record that substantially surpassed the corresponding normal monthly averages. These occurrences had several severe consequences, including urban flooding and landslides, which resulted in significant socioeconomic losses, loss of life, as well as disruption of many road and train connections [22], [37]–[39]. Using a proper pluvial flood model generated with the HEC-RAS software [40], flood depth maps for different return periods (2, 5, 10, 20, 50, 100, and 500 years) have been simulated for the area under study. The hydrological model was formulated using a digital elevation model (DEM) integrated with the STRM (Shuttle Radar Topography Mission) in QGIS [30], along with observed rainfall data for Lisbon [41]. The data acquired was used to generate the IDF curves (intensity-duration-frequency) for Lisbon, which served as a basis for calculating hydrographs according to the Soil Conservation Service-Curve Number (SCS-CN) method [42]. The hydrographs were then used as boundary conditions for the HEC-RAS rainfall model.

5. VULNERABILITY MODEL

Vulnerability can be defined as a measure of the consequences caused by a specific hazard. Vulnerability is often represented as a percentage of loss (ranging from 0 to 1) of a specific element at risk, [29]. Since the two hazards have independent metric systems, two separate approaches were used to compute the percentage of losses for seismic and flood vulnerability [2].

5.1. Seismic vulnerability

The seismic vulnerability of buildings was modelled using the index-based methodology proposed in the Risk-UE project [43]. In this methodology, a building typology is assigned to each building, starting from the Building Typology Matrix (BTM) proposed by the project, and the corresponding vulnerability index $\bar{V}_I$ is then calculated through the following equation:

$$\bar{V}_I = V_I^* + \Delta V_R + \Delta V_m \tag{2}$$

where V_I^* is the most probable value of the vulnerability index associated with the macroseismic building class; ΔV_R is the regional vulnerability factor i.e. a measure of how susceptible a region is to damage from a natural hazard. Specifically, the regional vulnerability factor ΔV_R considers the specific quality of certain building types at the regional level so, the vulnerability index is then adapted based on expert judgement or based on the observed vulnerability. Concerning, ΔV_m is intended as the sum of behaviour modifiers that alter the vulnerability index taking into account specific characteristics of the analysed building, i.e. the plan regularity, type of foundations, state of preservation and so on. All of these modifiers depend on the attributes of the structure as provided in [43]. Based on the features of Pombalino structures, the 324 Pombalino URM buildings were examined and assigned an M3.1 BTM class (i.e. wooden slabs URM with $V^*_{I,BTM}=0.74$) as reported in Table 1.

Table 1- M3.1 building vulnerability index from [43].

Category (BTM)	$V^{min}_{I,BTM}$	$V^{-}_{I,BTM}$	$V^{*}_{I,BTM}$	$V^{+}_{I,BTM}$	$V^{max}_{I,BTM}$
M3.1	0.46	0.65	0.74	0.83	1.02

After identifying the vulnerability index $\bar{V}_I$, the mean damage grade (μ_D) was estimated using a semi-empirical formulation that relates the expected mean damage, to the macroseismic intensity (I), as proposed by [44]. To gain insight into the expected consequences of the given scenario, 6 damage thresholds (D_k=0, 1, 2,..., 5) were chosen according to the EMS-98 damage scale [45]. The letter k represents the damage threshold, which ranges from 0 to 5: D0 (no damage); D1 (negligible damage); D2 (moderate damage); D3 (substantial damage); D4 (near collapse); D5 (collapse). Based on these assumptions, the probabilistic evaluation may be calculated in terms of both damage distributions and fragility curves. Consequently, to represent the damage scenario related to the building typology under consideration, a beta distribution function, $p_b(x)$, may be used, as suggested in [43]:

$$p_b(x) = \frac{\Gamma(t)}{\Gamma(t-r)} \cdot \frac{(x-a)^{r-1}(b-x)^{t-r-1}}{(b-a)^{t-1}}, \qquad a \leq x \leq b \tag{3}$$

where it is assumed that a=0; b=6; t=8 and $r = t\,(0.007\mu_D^3 - 0.052\mu_D^2 + 0.2875\,\mu_D)$. The discrete damage distribution was then calculated as follows:

$$p_k = P_\beta\,(k+1) - P_\beta\,(k) \tag{4}$$

The typological fragility curves (see Fig. 3) were obtained directly from the cumulative probability beta distribution as follows:

$$P\,(D \geq D_k) = 1 - P_\beta\,(k) \tag{5}$$

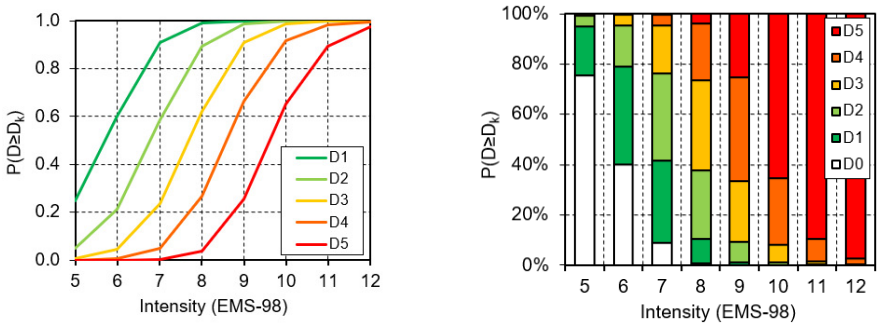

a) b)

Fig. 3 – Vulnerability estimation: a) Fragility curves for M3.1 typology and b) corresponding discrete damage distribution.

5.2. Flood vulnerability

The proposed study adopted the stage-damage curves reported by [46] which allowed to assess the damage by classifying the structures with or without a basement and with two or fewer floors and three or more floors. Furthermore, according to [2], it was assumed that for a water level less than 0.25m, no damage is experienced by the buildings. Indeed, due to the variable ground elevations in the area, 0.25m represents the average height of the building's entry door above the road level. Thus, as an indicative example a worst-case scenario, i.e. 500-year, for the Baixa Pombalina are shown in Fig. 4.

2.5

a) b)

Fig. 4 – Flood vulnerability estimation for a return period of 500 years: a) Water depth; b) Flood damage.

It is worth noting that water levels rising beyond 2.5 meters can be attributed to the simulated rainfall flooding. These floods are triggered by heavy rainfall, causing a gradual increase in the gradient of water levels based on the area's topography. This phenomenon continues until buildings are inundated.

6. MULTI-RISK MODEL

The multi-risk assessment was carried out with the two hazards considered independent (i.e. with no interactions). As a result, the entire risk may be considered as the sum of earthquake and flood losses, which might represent the condition where two separate events occur within a short period [21]. The total seismic building losses were determined by multiplying the monetary exposure by the damage levels reached by the structures in the simulated scenario. The monetary exposure (E_i) is equivalent to the value derived by equation (1) (refer to Section 3), whereas the damage level (D_i= 1, 2,...5) indicates the extent of losses (D%) experienced by the building as provided by [47] and reported in Table 2.

Table 2- Earthquake building losses depicted according to [47].

Damage level (D_k)	% Cost of Replacement
D0	0%
D1	1%
D2	20%
D3	40%
D4	80%
D5	100%

Consequently, the global losses represent a smaller percentage of the total reconstruction cost, estimated to be equivalent to the market value due to a lack of available data. The calculation of total flood building losses involved multiplying the monetary exposure (E_i) by the physical damage derived from the stage-damage curves (D%) [46] as reported in Figure 5.

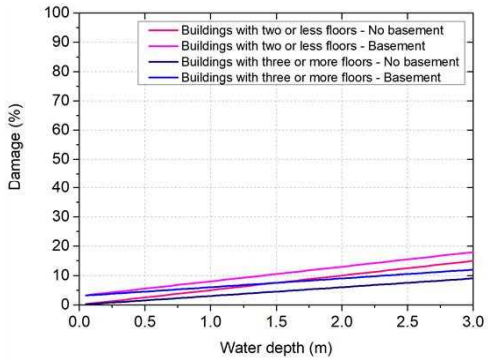

Fig. 5 – Stage-damage curves adopted from [46].

The Loss Exceedance Curves (see Fig. 6) relate expected losses to the corresponding mean annual frequency of exceedance of a given hazard (Fig. 6a) and the return period (Fig. 6b), through the following formulation [21]:

$$\mathrm{v}(\mathrm{p}) = \sum_{\mathrm{i}=1}^{\mathrm{Events}} \Pr(\mathrm{P} > \mathrm{p} \mid \mathrm{Event_i}) \cdot \mathrm{F_A}(\mathrm{Event_i}) \tag{6}$$

where $\mathrm{v}(\mathrm{p})$ is the exceedance rate of loss, p; $\mathrm{F_A}(\mathrm{Event_i})$ is the annual frequency of occurrence of the $\mathrm{Event_i}$; and $\Pr(\mathrm{P}>\mathrm{p} \mid \mathrm{Event_i})$ is the probability of the loss to be greater than or equal to p, conditioned by the occurrence of $\mathrm{Event_i}$.

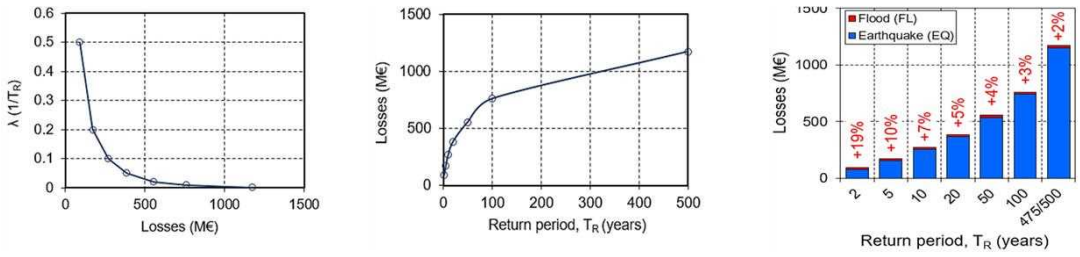

a) b) c)

Fig. 6 – Multi-hazard curves: a) Loss-Annual exceedance; b) Loss-Return periods and c) dependency damage increment induced by floods.

The multi-hazard curve, as illustrated in Figure 6b, implies that larger return periods result in higher building losses. For example, for a 500-year scenario, building losses are around 1150 M€ for earthquakes and 21 M€ for floods, but for a 2-year return period, earthquake losses are approximately 76 M€ and flood losses are 14 M€. Subsequently, Figure 6c depicts the correlation of how the flood damage contributes to the increase of corresponding seismic damage. This analysis illustrates the extent to which flood-related losses increase earthquake losses for different return periods. In cases where both hazards occur nearby, flood losses enhance seismic losses by approximately 7%-20% for return periods of 2, 5, and 10 years. However, for longer return periods (20, 50, 100, 475/500 years), the increment is around 2%-5%. These data are essential for a comprehensive assessment of potential losses due to the hazards under consideration, providing valuable insights to better understand strategies for risk reduction.

7. CONCLUSION

This research introduces a multi-risk model for Lisbon, considering the vulnerabilities posed by both seismic and rainfall-induced flood hazards. Much like numerous urban areas globally, Lisbon has encountered various perils that jeopardize its inhabitants, infrastructure, and economic well-being. This particular study concentrates on evaluating typical unreinforced masonry (URM) structures situated within a specific area known as Baixa Pombalina. The ensuing section outlines the key findings derived from this study:

- The exposure model, utilising remote sensing and GIS data, provides crucial information about the characteristics of the surveyed buildings. Notably, it reveals that 82% of these buildings are of the Pombalino type, while 18% are constructed with reinforced concrete. The majority, accounting for 96% of the sample, consist of buildings with 5-7 floors. In terms of condition, 53% are in good or very good condition, while 42% are in moderate to very poor condition. These buildings have different positions, with 58% in intermediate positions, 37% in corner locations, and 5% at head positions.
- The outcomes obtained through the Risk-UE method indicate that 75% of URM buildings possess a vulnerability index (V_I) exceeding 0.8 (very high vulnerability). Meanwhile, 25% of these buildings exhibit V_I values falling within the range of 0.6 to 0.8, signifying a high vulnerability. For a return period of 475 years, the damage distribution is as follows: 38% of buildings are classified as D3 (with damage levels between 2 and 3), 57% fall into the D4 category (damage levels ranging from 3 to 4), and the remaining 5% are categorized as D5 (with damage levels between 4 and 5);
- Regarding the flood scenario, vulnerability assessment relied on stage-damage curves sourced from existing literature. In the context of a 500-year return period, it was found that 61% of unreinforced masonry (URM) buildings experienced water depths below 0.25 meters, while only 4% encountered depths exceeding 2.50 meters;
- For a 475/500-year return period, the estimated seismic building losses were approximately €1150 million and €21 million the flood losses. The higher earthquake losses can be attributed to a larger proportion of structural damage compared to the

damage that floods normally generate, which is, in mostly, related to contents. Future research could explore this further by considering content damage. Regarding the increase in damage, it's noteworthy that flood events boost seismic losses by approximately 7%-20% for return periods ranging from 2 to 10 years, while the increase is notably lower (2%-5%) for longer return periods (ranging from 20 to 500 years).

The methodology herein proposed offers a well-structured framework for prioritizing future risk reduction efforts in urban areas to effectively confront potential threats. This methodology brings several advantages, including improved decision-making processes, the targeted allocation of resources to reduce specific risks and the reinforcement of community preparedness and resilience. Ultimately, the adoption of this methodology plays an important role in minimizing the potential impacts of future risks, while simultaneously fostering sustainable and resilient urban development. However, it is essential to point out the limitations of the study, notably the absence of a model addressing interactions among the examined hazards. The presented data should be considered as an initial phase, with the potential for a more comprehensive risk analysis in the future. An enhancement could involve integrating a multi-criteria analysis to manage probabilistic dependencies among hazards and assess their combined impacts. Moreover, in the absence of information on reconstruction costs in the study area, the conducted analysis, while conservative, takes into account the reduction in the market value of assets exposed to risk due to the impact of the two considered hazards.

8. ACKNOWLEDGEMENT

This work was partly financed by FCT / MCTES through national funds (PIDDAC) under the R&D Unit Institute for Sustainability and Innovation in Structural Engineering (ISISE), under reference UIDB / 04029/2020, and under the Associate Laboratory Advanced Production and Intelligent Systems ARISE under reference LA/P/0112/2020. The third author would also like to thank the financial support of the Base Funding - UIDB/04708/2020 of CONSTRUCT - Instituto de I&D em Estruturas e Construções, funded by national funds through FCT/MCTES (PIDDAC).

9. REFERENCES

[1] Julià, P. B. and Ferreira, T. M. (2021) From single-to multi-hazard vulnerability and risk in Historic Urban Areas: A literature review. *Natural Hazards*, **108**(1), 93–128. https://doi.org/10.1007/s11069-021-04734-5

[2] Arrighi, C. Tanganelli, M. Cristofaro, M. T. Cardinali, V. Marra, A. Castelli, F. and De Stefano, M. (2022) Multi-risk assessment in a historical city. *Natural Hazards*, 1-32.

[3] McGlade, J. Bankoff, G. Abrahams, J. Cooper-Knock, S. Cotecchia, F. Desanker, P. Erian, W. Gencer, E. Gibson, L. and Girgin, S. (2019) *Global assessment report on disaster risk reduction 2019*. https://gar.undrr.org/sites/default/files/reports/2019-05/full_gar_report.pdf

[4] UNISDR. (2009). *Terminology on disaster risk reduction*. Geneva, Switzerland. www. unisdr.org/files/7817_UNISDRTerminologyEnglish.pdf

[5] Grünthal, G. Thieken, A. H. Schwarz, J. Radtke, K. S. Smolka, A. and Merz, B. (2006) Comparative risk assessments for the city of Cologne–storms, floods, earthquakes. *Natural Hazards*, **38**, 21–44.

[6] Kappes, M. S. Keiler, M. Von Elverfeldt, K. and Glade, T. (2012) Challenges of analyzing multi-hazard risk: A review. *Natural Hazards*, **64**, 1925–1958.

[7] Johnson, K. Depietri, Y. and Breil, M. (2016) Multi-hazard risk assessment of two Hong Kong districts. *International Journal of Disaster Risk Reduction*, **19**, 311–323.

[8] Gallina, V. Torresan, S. Critto, A. Sperotto, A. Glade, T. and Marcomini, A. (2016) A review of multi-risk methodologies for natural hazards: Consequences and

challenges for a climate change impact assessment. *Journal of Environmental Management*, **168**, 123–132.
[9] De Angeli, S. Malamud, B. D. Rossi, L. Taylor, F. E. Trasforini, E. and Rudari, R. (2022) A multi-hazard framework for spatial-temporal impact analysis. *International Journal of Disaster Risk Reduction*, **73**, 102829.
[10] UNEP. (1992). *AGENDA 21*. In: United Nations Conference on Environment & Development, 3 to 14 June 1992, Rio de Janerio, Brazil, 1355 United Nations Environment Programme, 1992. https://sustainabledevelopment.un.org/content/documents/Agenda21.pdf
[11] UN. (2002). *Report of the World Summit on Sustainable Development, 26 August—4 September 2002, Johannesburg, South Africa, United Nations, 2002*. https://digitallibrary.un.org/record/478154
[12] UNISDR. (2005). *Hyogo framework for action 2005–2015: Building the resilience of nations and communities to disasters*. 380.
[13] UNISDR. (2015). Sendai framework for disaster risk reduction 2015–2030. 1. https://www.unisdr.org/files/43291_sendaiframeworkfordrren.pdf
[14] Sesana, E. Gagnon, A. S. Bertolin, C. and Hughes, J. (2018) Adapting cultural heritage to climate change risks: Perspectives of cultural heritage experts in Europe. *Geosciences*, **8**(8), 305.
[15] Ciurean, R. Gill, J. Reeves, H. J. O'Grady, S. and Aldridge, T. (2018) Review of multi-hazards research and risk assessments (Open Report OR/18/057). *British Geological Survey*, https://nora.nerc.ac.uk/id/eprint/524399
[16] Tilloy, A. Malamud, B. D. Winter, H. and Joly-Laugel, A. (2019) A review of quantification methodologies for multi-hazard interrelationships. *Earth-Science Reviews*, **196**, 102881.
[17] El Morjani, Z. E. A. Ebener, S. Boos, J. Abdel Ghaffar, E. and Musani, A. (2007) Modelling the spatial distribution of five natural hazards in the context of the WHO/EMRO Atlas of Disaster Risk as a step towards the reduction of the health impact related to disasters. *International Journal of Health Geographics*, **6**(1), 1–28.
[18] Barrantes, G. (2018) Multi-hazard model for developing countries. *Natural Hazards*, **92**(2), 1081–1095.
[19] Lee, K. H. and Rosowsky, D. V. (2006) Fragility analysis of woodframe buildings considering combined snow and earthquake loading. *Structural Safety*, **28**(3), 289–303.
[20] Petrone, C. Rossetto, T. Baiguera, M. De la Barra Bustamante, C. and Ioannou, I. (2020) Fragility functions for a reinforced concrete structure subjected to earthquake and tsunami in sequence. *Engineering Structures*, ***205***, 110120.
[21] Tocchi, G. Ottonelli, D. Rebora, N. and Polese, M. (2023) Multi-Risk Assessment in the Veneto Region: An Approach to Rank Seismic and Flood Risk. *Sustainability*, **15**(16), 12458.
[22] Trigo, R. M. Ramos, C. Pereira, S. S. Ramos, A. M. Zêzere, J. L. and Liberato, M. L. R. (2016) The deadliest storm of the 20th century striking Portugal: Flood impacts and atmospheric circulation. *Journal of Hydrology*, **541**, 597–610.
[23] Bernardo, V. Sousa, R. Candeias, P. Costa, A. and Campos Costa, A. (2021) Historic appraisal review and geometric characterization of old masonry buildings in Lisbon for seismic risk assessment. *International Journal of Architectural Heritage*, **16**(12), 1921–1941.
[24] Martins, A. N. Forbes, C. Pereira, A. A. and Matos, D. (2018) The changing city: Risk and built heritage. The case of Lisbon downtown. *Procedia Engineering*, **212**, 921–928.
[25] Barchetta, L. Petrucci, E. Xavier, V. and Bento, R. (2023) A Simplified Framework for Historic Cities to Define Strategies Aimed at Implementing Resilience Skills: The Case of Lisbon Downtown. *Buildings*, **13**(1), 130.
[26] Google Earth. (n.d.). *https://www.google.it/earth/*. Accessed 27 September 2023.
[27] Catulo, R. Falcão, A. P. Bento, R. and Ildefonso, S. (2018) Simplified evaluation of seismic vulnerability of Lisbon Heritage City Centre based on a 3DGIS-based methodology. *Journal of Cultural Heritage*, *32*, 108–116.

[28] UN. (2016). *Report of the open-ended intergovernmental expert working group on indicators and terminology relating to disaster risk reduction*. United Nations General Assembly: New York, NY, USA, 41.
[29] Sterlacchini, S. Akbas, S. O. Blahut, J. Mavrouli, O.-C. Garcia, C. Luna, B. Q. and Corominas, J. (2014) Methods for the characterization of the vulnerability of elements at risk. *Mountain Risks: From Prediction to Management and Governance, Springer Dordrecht*, 233–273.
[30] Graser, A. (2013) *Learning QGIS 2.0*. Packt Publishing Ltd.
[31] Instituto Nacional de Estatística, IP - Portugal. (n.d.). https://www.ine.pt/xportal/xmain?xpid=INE&xpgid=ine_base_dados. Accessed 20 July 2023.
[32] Calvi, G. M. Pinho, R. Magenes, G. Bommer, J. J. Restrepo-Vélez, L. F. and Crowley, H. (2006) Development of seismic vulnerability assessment methodologies over the past 30 years. *ISET Journal of Earthquake Technology*, **43**(3), 75–104.
[33] Teves-Costa, P. Batllo, J. and Cabral, J. (2017) The Lower Tagus Valley (Portugal) earthquakes: Lisbon 26 January 1531 and Benavente 23 April 1909. *Física de La Tierra*, **29**(2017), 61–84.
[34] Sá, L. Morales-Esteban, A. and Durand Neyra, P. (2018) The 1531 earthquake revisited: Loss estimation in a historical perspective. *Bulletin of Earthquake Engineering*, **16**, 4533–4559.
[35] Vilanova, S. P. and Fonseca, J. F. B. D. (2007) Probabilistic seismic-hazard assessment for Portugal. *Bulletin of the Seismological Society of America*, **97**(5), 1702–1717.
[36] Lantada, N. Pujades, L. G. and Barbat, A. H. (2018) Earthquake risk scenarios in urban areas: A review with applications to the Ciutat Vella District in Barcelona, Spain. *International Journal of Architectural Heritage*, **12**(7–8), 1112–1130.
[37] Fragoso, M. Trigo, R. M. Zêzere, J. L. and Valente, M. A. (2010) The exceptional rainfall event in Lisbon on 18 February 2008. *Weather*, **65**(2), 31–35.
[38] Liberato, M. L. R. Ramos, A. M. Trigo, R. M. Trigo, I. F. Durán-Quesada, A. M. Nieto, R. and Gimeno, L. (2012) Moisture sources and large-scale dynamics associated with a flash flood event. *In: Lin, J., Brunner, D., Gerbig, C., Stohl, A., Luhar, A., Webley, P. (Eds.), Lagrangian Modeling of the Atmosphere*, **200**, 111–126.
[39] Leal, M. Ramos, C. and Pereira, S. (2018) Different types of flooding lead to different human and material damages: The case of the Lisbon Metropolitan Area. *Natural Hazards*, **91**(2), 735–758.
[40] Hydrologic Engineering Center. (2021). *HEC-RAS 2D Modeling User's Manual*. U.S. Army Corps of Engineers, Davis CA.
[41] Brandão, C. Rodrigues, R. and Costa, J. P. (2001) *Análise de fenómenos extremos precipitações intensas em Portugal continental*. Direcçao dos serviços de recursos hıdricosdo Instituto da Água, Lisboa, https://snirh.apambiente. pt/snirh/download/relatorios/relatorio_prec_intensa.pdf
[42] SCS. (1993). *Hydrology. National Engineering Handbook*. USDA.
[43] Milutinovic, Z. V. and Trendafiloski, G. S. (2003) *Risk-UE An advanced approach to earthquake risk scenarios with applications to different european towns*. Contract: EVK4-CT-2000-00014, WP4: Vulnerability of Current Buildings, 1–111.
[44] Lagomarsino, S. and Giovinazzi, S. (2006) Macroseismic and mechanical models for the vulnerability and damage assessment of current buildings. *Bulletin of Earthquake Engineering*, **4**(4), 415–443.
[45] Grünthal, G. (1998) *European macroseismic scale 1998*. European Seismological Commission (ESC).
[46] Dias, L. Braunschweig, F. Grosso, N. Costa, H. and Garrett, P. (2010) *Flood risk mapping. Methodological guide.*
[47] Roca, A. Goula, X. Susagna, T. Chávez, J. González, M. and Reinoso, E. (2006) A simplified method for vulnerability assessment of dwelling buildings and estimation of damage scenarios in Catalonia, Spain. *Bulletin of Earthquake Engineering*, **4**(2), 141–158.